Measurement: Sensors 24 (2022) 100483

Contents lists available at ScienceDirect

Measurement: Sensors

journal homepage: www.sciencedirect.com/journal/measurement-sensors

# Development of a multi-modal sensor network to detect and monitor knee joint condition

I. Vatolik [a,*], M. Everington [a], G. Hunter [a], N. Swann [b], A.T. Augousti [a]

[a] Faculty of Engineering, Computing and the Environment, Kingston University London, KT1 2EE, UK
[b] Faculty of Health and Medical Sciences, University of Surrey, GU2 7XH, UK

ARTICLE INFO

*Keywords:*
Acoustic emissions
Knee joint
Osteoarthritis

ABSTRACT

Osteoarthritis is a major cause of mobility problems in older people and is a particular problem in former sportspeople. The objective of this study was to develop and characterise a new system for the detection, monitoring and analysis of acoustic emissions from knee joints. 15 adult volunteers participated in the study. The participants performed six sets of three sit-stand-sit cycles. Reflective markers were placed at specific body landmarks recorded by 3D cameras. The exercise was performed with one foot on a force platform. A sensitive condenser microphone with a wide frequency response was connected to a dedicated acoustic analysis unit. Preliminary results provide clear acoustic signals showing a distinctive sequence of impulse-decay forms occurring naturally during each sit-stand-sit cycle. There are distinct differences between the acoustic signals emitted from younger healthy knees and those from aged knees. This work demonstrates the potential for this system to be used as an indication of the state of health of a human knee during movement.

## 1. Introduction

The prevalence of injuries associated with dynamic physical activity has compelled scientists to study changes in body structures after exercise, with degenerative changes to tissues and implications of these of particular concern [1–3]. The function of cartilage in joints is for bones in motion to evenly transmit loads from one body segment to another at very low frictions [4]. During these events it has been shown that cartilage undergoes changes in volume, thickness, and joint space narrowing [5].

Osteoarthritis (OA) is a chronic condition of the synovial joint and is the result of thinning or loss of cartilage. Since the cartilage cushions the ends of the bones, its loss causes a reduced joint space and sometimes the bone ends come into direct contact with each other. Knee joints produce sound during motion and different acoustic frequencies will be produced when the cartilage begins to thin.

Some studies have identified the risk factors associated with potential causes of OA, including a raised body mass index (BMI), female gender and risk factors resulting from manual work [6,7]. Furthermore, participation in elite sports and history of previous knee injuries also have the potential to cause this degenerative knee joint disease [8]. performed a retrospective review of the US military population. Due to the extreme physical training of servicemen and servicewomen and the thorough health screening for preexisting conditions, this population was selected for epidemiological studies researching the development of primary and secondary OA. The research revealed that 70% of failed Army Physical Examinations are due to arthritis, of which 94.4% occurred subsequent to previous trauma to the knee.

Despite advances in imaging technology there is a lack of equipment that could be used to investigate the behaviour of cartilage and assess the functional components of the knee performing under a variety of movements and loading. Although dynamic magnetic resonance imaging (MRI), X-Ray and ultrasound are used with excellent accuracy, in the home or clinical setting it is impractical because of cost, portability and accessibility. Structures and materials under load are known to generate acoustic emissions (AE) [9]. In recent years several studies have investigated the use of vibroarthrography and acoustic emission recording techniques as a means to detect and monitor knee conditions at different stages of joint degenerative disease. The AE and VAG signals of knee joints were recorded using piezoelectric transducers and stethoscopes and found that OA knees produce more acoustic events with longer durations and higher amplitudes than healthy knees [10–12].

In 2010, Shark et al. [37] used AE as a non-invasive biomarker to identify and assess joint degeneration. Their study used a piezo-electric

* Corresponding author.
*E-mail address:* k1465290@kingston.ac.uk (I. Vatolik).

https://doi.org/10.1016/j.measen.2022.100483
Received 27 July 2021; Received in revised form 22 September 2022; Accepted 22 September 2022
Available online 30 September 2022

**Table 1**
Participants' age (n = 15) and gender distribution.

| Age Category | Participants | Age |
|---|---|---|
| **18–34 (m)** | 4 | 27 ± 5 |
| **35–49 (m)** | 4 | 45.5 ± 4.5 |
| **50+ (m)** | 2 | 51.5 ± 0.5 |
| **18–34 (f)** | 4 | 24 ± 5 |
| **35–49 (f)** | 1 | 43 |
| **50+ (f)** | 0 | n/a |

transducer to measure the frequency of AE signals. The results of this study showed significant differences between the acoustic frequencies of a healthy population and an older osteoarthritic population [10]. also investigated the differences in acoustic emission between healthy and OA knees and found that healthy knees produce substantially fewer AE events with lower peak magnitude and average signal level values than OA knees. Since AE can recognise changes in acoustic frequencies that could be associated with functional changes to joints, it could be used to identify development and progression of OA in its early stages [13]. demonstrated that the knee joint AE events can be picked up not only by a piezo-electric transducer directly attached to the knee but also by a commercially available air microphone. They argued that even though contact microphones are used with great accuracy in lab settings, patients in home settings might, due to their inexperience, incorrectly attach the microphones and get erroneous readings. Therefore, they conducted research investigating the consistency of the air microphones and reported that air microphones obtained higher quality signals than microphones attached to the skin (with a signal-to-noise ratio of 12.4 dB versus 8.4 dB).

As suggested by previous research [3,14–17], highly repetitive loading can with time deplete the joint of glycoproteins which serve as lubricants and wear away the cartilage. During any form of physical activity involving the lower extremities, interstitial hydrostatic fluid initially supports the pressure build up within the tissue. Then the fluid is redistributed within the matrix. Because of this the cartilage begins to deform and as the hydrostatic pressure gets close to zero the load rests just on the cartilage [4,18]. Since the knee joint generates sound and vibrations during motion, a knee with deformed cartilage will generate different sound frequencies [19].

Vibroarthrography (VAG) is a method of recording vibration and sound emission from knee joint during motion. The equipment used to record these events (typically accelerometers, stethoscopes or piezo-electric transducers) is placed at articular surfaces [20]. In 1987 McCoy et al. [32] reported that characteristic signals were produced in most patients with meniscal injuries (86%), which suggests that early cartilage degradation could be identified by alteration of the healthy joint crepitus. They furthermore demonstrated the possibility of using knee sound analysis to identify meniscal lesions, chondromalcia patella and arthritis. This was performed by categorising sound peaks into frequency groups [21]. followed up on this work and created VAG profiles for meniscal lesions and chondromalacia patella. He reported that meniscal lesions showed sharp bursts in the AE signal. It presented itself as a short duration energy burst in the range 0–200 Hz in the spectral contour plots. Mild chondromalacia patella appeared as a long duration activity in the frequency range 0–300 Hz, whilst severe chondromalacia was observed at relatively low frequencies (a range of 0–100 Hz). This was due to the loose cartilage elements between the rubbing surfaces.

The articular cartilage in the knee joint undergoes significant changes in volume during exercising [1–3]. To transfer the loads evenly from one body part onto another, cartilage provides surfaces that allow bones to glide with low friction. At first the load is supported by the interstitial hydrostatic fluid pressure; then the fluid spreads across the matrix and cartilage starts to deform. After the fluid flow ceases the entire weight is supported by the proteoglycan-collagen cartilage matrix [4]. The study conducted by Ref. [3] used an MRI to monitor deformation and recovery of the cartilage after a 20-km run. The results show that the cartilage deformed by −7% and after a 60-min rest period recovered by 5.3% [1]. reported similar results to the above-mentioned study; this research investigated cartilage deformation after 50 and 100 knee bends and its recovery after a 90-min period of rest. The volume of cartilage reduction was reported to be between −2.4% and −8.6% and showed no significant differences between the two conditions (see Table 1). However [1], showed that the joint cartilage fully recovered after 90-min of rest.

The longer-term aim of this study is to determine whether a proprietary Laryngograph DSP Unit and a sensitive condenser microphone with a wide frequency response could be used as a non-invasive method for monitoring knee joint cartilage degeneration and deformation and to

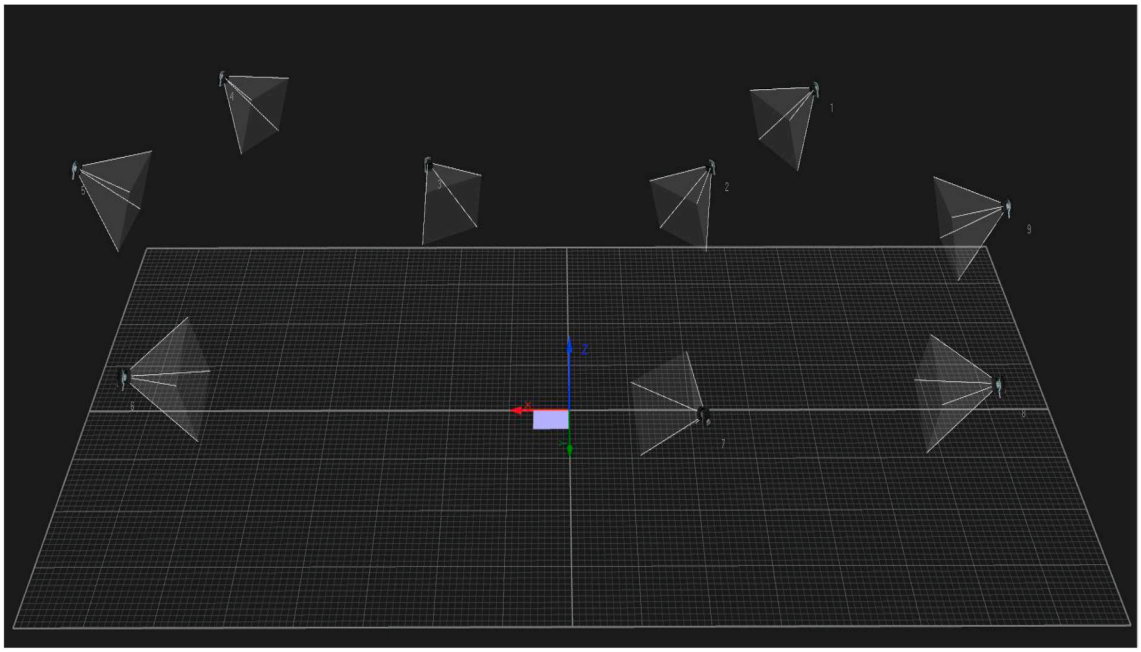

**Fig. 1.** A screenshot from the QTM software of the 3D cameras set up around the force plate.

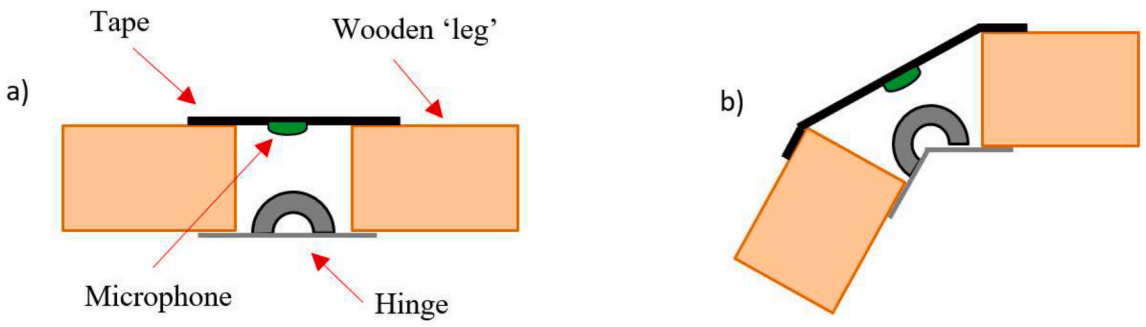


**Fig. 2.** Illustration of the knee phantom with the microphone attached to the tape. a) The starting point when the tape and the microphone were attached; b) The point of maximum stretch of the tape.

determine whether this dedicated sound analysis system could be used as a tool to identify osteoarthritis.

Conducting this research has involved developing a unique device with a dedicated sound analysis system designed to recognise low frequency acoustic events. Designing such a device and exploring its potential could greatly aid athletes performing at all levels to reduce or possibly avoid sustaining wear and tear injuries to the cartilage in any joint.

Previous studies established that cartilage deforms after physical activity and returns to normal as soon as 90 min after exercising as noted above [1,3,5]. Due to this phenomenon, it can be hypothesized that the sound frequency generated by the knee joint will vary before and immediately after exercising and after a resting period.

The aim of this initial work, therefore, is to validate the use of a microphone with a dedicated sound analysis system as a tool for assessing the integrity of knee joints using acoustic emission and to validate repeatable acquisition of acoustic emission signals of knee joints and standardise the sit-stand-sit protocol. Furthermore, we have sought to develop appropriate data analysis protocols in order to extract the most relevant information from the signals in order that different test groups, and also measurements from longitudinal studies on specific subjects, may be meaningfully compared.

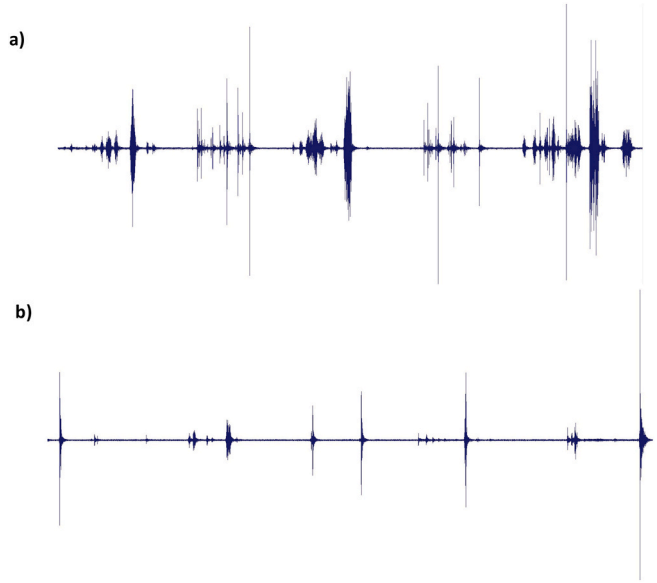


**Fig. 3.** Signal from a) KT Kinesiology tape b) Hypafix Transparent tape.

## 2. Methodology

### 2.1. Data acquisition

Experiments were carried out on 15 adult volunteer participants of both sexes and of varied age groups (see Table 1). These were randomly recruited from the population of Kingston University London staff and students. Each of these was informed of the nature of the project and experiment, and of their right to withdraw from it at any point, before the start of the experiment, and had given their written consent to proceed. This research project and its methodology were granted ethical approval by the Ethics Committee of Kingston University London. To protect the privacy of the participants, the collected data were anonymised, coded, and processed only by researchers who were involved in the project. All the data was stored and processed in accordance with GDPR guidelines.

#### 2.1.1. Biomechanics equipment

The participant data indicates that a gender comparison is not strictly appropriate given the more limited number of female participants, noting further that the aim of this paper is to establish the development of processing techniques that highlight correlation of the signal with kinematic variables. Data on additional subjects will be added in due course which will permit a more reliable comparison between the subject groups and we hope to report results of this comparison in future work following the successful validation of this technique.

Nine 3D Oqus 700+ Series cameras (Qualysis MedicalAB, Sävedalen, Sweden) were positioned around the capture volume (see Fig. 1), calibrated using the manufacturer recommended static and dynamic methods and. used to record the motion of retroreflective markers at 200Hz. This calibration method is performed by a measurement procedure in the motion tracking software Qualisys Track Manager (QTM) to accurately calculate 3D data. The L-frame for 3D calibration was positioned on the bottom right corner of the force plate (the point of origin of the capture volume) and a 600 mm carbon fiber wand with spherical markers was used. For high-quality data, the average residual should be below 1 mm. The average residual is the number of points used in the calculation of the distance between the origin of the coordinate system to the optical center of the camera. To record ground reaction forces the participants performed movements standing with one leg on the floor and the other leg (with microphone attached) on the Multicomponent Kistler Force Plate 9281CA (Kistler Instruments Ltd., London, UK). The force platform (FP) recorded at a frequency of 2000 Hz. The collected dynamic data was not used in this study, which sought primarily to correlate acoustic emission with kinematic data, but it is planned to be analysed later in combination with the kinematic data to gain further insight into the causes and correlations of knee joint AE.

#### 2.1.2. Acoustic emission system

A sensitive condenser microphone with a frequency range of 100 Hz

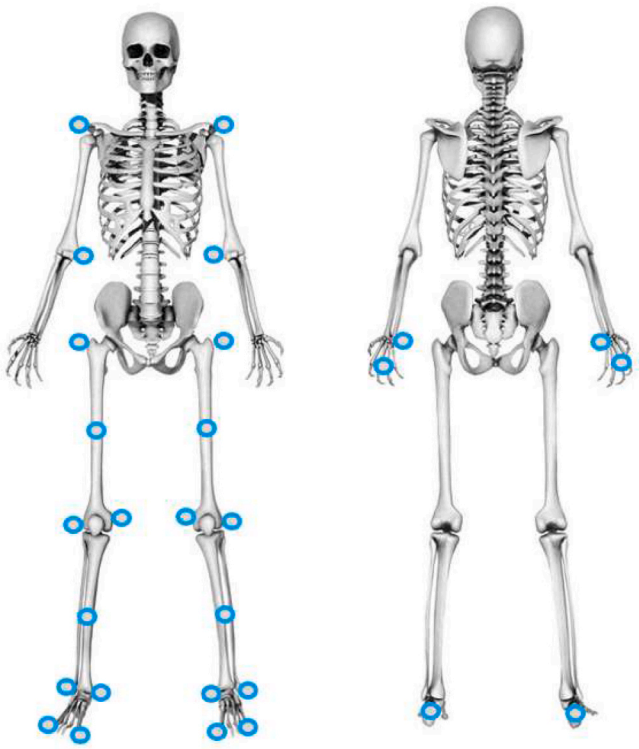

**Fig. 4.** The image shows the placement of the reflective markers on the body landmarks.

to 4.7 kHz (Knowles MR-28406-000, Knowles Electronics, IL, USA), was connected to the Laryngograph DSP Unit recording at 16,000 Hz. The Speech Filing System (University College London, UK) software was used to operate the Laryngograph DSP Unit (Laryngograph Ltd., London, UK). It is a computing environment that is used to study the nature of speech.

The microphone was attached on the lateral soft part of the knee, below the patellofemoral joint, using 15 cm × 10 cm patches of Hypafix Transparent Dressing. A small incision was made in each tape for convenient microphone application and to avoid the wire being applied to the skin. To avoid any unnecessary noise, the area of application was shaved, abraded, cleaned with an alcohol wipe and a small amount of clear conductive gel was applied. For increased tension on the microphone the dressing was applied on the extended knee joint.

Three types of tape were tested for noise emission using a phantom imitating a knee joint. The phantom consisted of a door hinge with two wooden rectangles attached to each end of the hinge. Each of the tapes was attached to both ends of the phantom with the microphone applied between the 'legs' of the phantom and above the hinge (see Fig. 2). The three types of tape were Hypafix Hypoallergenic Dressing Tape 10 cm × 10 cm, Leukotape Kinesiology Tape 5 cm × 10 cm and Hypafix.

Transparent Dressing 15 cm × 10 cm. The latter emitted the smallest number of acoustic events and with the smallest magnitude (see Fig. 3). Therefore, this tape was selected for testing.

### 2.1.3. *Procedures*

28 retroreflective markers were placed on bony anatomical landmarks and specific parts of the body (1st and 5th metatarsal, calcaneus, medial and lateral malleolus, shank, medial and lateral epicondyle of femur, thigh, greater trochanter, acromio-clavicular joint, lateral condyle of humerus, styloid process of ulna, head of the third metacarpal) for identification in the motion tracking software Qualisys Track Manager (QTM) (see Fig. 4).

Each participant was asked to perform a set of three sit-stand-sit (S–S–S) cycles three times for each leg. Each S–S–S movement had an ascending phase (from the chair to fully erect position) and a descending phase (from fully erect position back to the chair). To lessen the effects of movement strategies the participants crossed their arms over their chest. Furthermore, a chair with a backrest and without an armrest was used. They were asked to perform this protocol on five different days over a period of three weeks from the commencement of their participation. This was to minimise variability due to potential gradual deterioration of the knee joint over a single prolonged period of investigation.

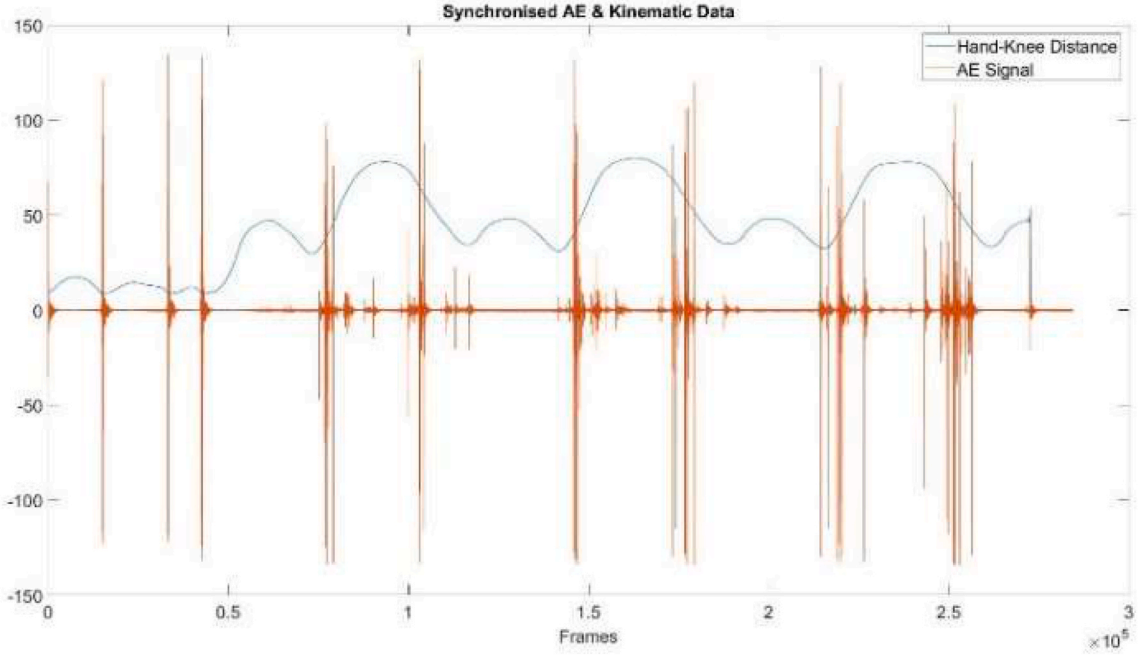


**Fig. 5.** A graph showing an example of synchronised acoustic data and resampled kinematic data.

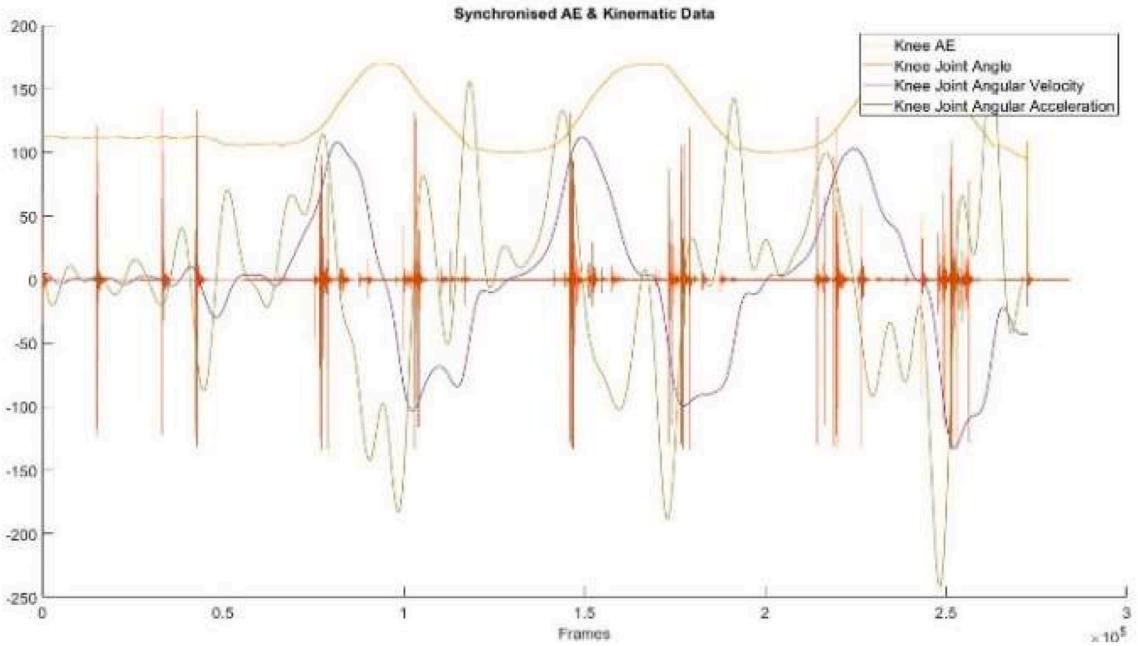


**Fig. 6.** This figure shows synchronised AE signal with kinematic data (θ, $\omega_n$, and$\alpha_n$).

### 2.2. Data processing

#### 2.2.1. AE and kinematic data synchronisation

Since the dynamic and kinematic data were recorded using QTM and the acoustic signals were recorded using a Speech Filing System (SFS), the data had to be manually synchronised prior to any data analysis. To synchronise the acoustic data with the kinematic and dynamic data participants were asked to perform four 'taps' on the microphone which were detected by both the QTM and the SFS. A custom-made MATLAB code was developed to first calculate the distance between hand and knee marker $d_{HK}$. The minimum distance in the quantity $d_{HK}$ would indicate contact between the hand and knee and hence contact with the microphone. This was calculated from the kinematic data using the following equation:

$$d_{HK} = \sqrt{\left(\vec{H} - \vec{K}\right)^2}$$

where $\vec{H}$ and $\vec{K}$ are the position vectors of the hand and knee marker coordinates, respectively. Upon contact with the microphone a significant spike in the acoustic signal is recorded. Once the first peak in the acoustic signal was aligned with the first minimum distance of $d_{HK}$ the two curves were successfully synchronised (see Fig. 5). The synchronisation of the kinematic variables of the knee calculated below was performed from the same frame as $d_{HK}$. This is because the data was calculated from the same footage recorded by the same motion tracking software (QTM). Due to the different recording frequencies of the 3D cameras (200 Hz) and the microphone (16,000 Hz), the kinematic data had to be upsampled using interpolation. The effective recording frequency was thus increased by a factor of 80.

#### 2.2.2. Calculations of kinematic variables of the knee joint

To fully investigate the features of the AE signal in relation to the kinematic variables such as knee angle, angular velocity and acceleration had to be calculated. To calculate the angle of the knee joint, only a subset of the acquired marker co-ordinate data was required, specified as follows. The leg segments thigh ($\overrightarrow{Thigh}$) and shank ($\overrightarrow{Shank}$) were created by subtracting leg marker coordinates:

$$\overrightarrow{Thigh_n} = GT_{xyz} - K_{xyz} = (GTx_n, \quad GTy_n, \quad GTz_n) - (Kx_n, \quad Ky_n, \quad Kz_n)$$

$$\overrightarrow{Shank_n} = K_{xyz} - A_{xyz} = (Kx_n, \quad Ky_n, \quad Kz_n) - (Ax_n, \quad Ay_n, \quad Az_n)$$

where $GT_{xyz}$, $K_{xyz}$ and $A_{xyz}$ are the 3D coordinates of the markers placed on the greater trochanter, lateral epicondyle of the femur and the lateral malleolus, respectively. The knee angle ($\theta$) was calculated in degrees using the inverse tangent of the cross and dot product of the thigh and shank segments:

$$\theta = arctan\left(\frac{\left|\overrightarrow{Thigh} \times \overrightarrow{Shank}\right|}{\overrightarrow{Thigh} \bullet \overrightarrow{Shank}}\right) * \frac{180}{\pi}$$

The angular velocity is defined as the rate of change of angular position with respect to time. Therefore, the instantaneous angular velocity of the knee for the nth sample in the data sequence ($\omega_n$) is calculated as a derivative of the $\theta$. In other words it is defined as the change in angle divided by the change in time:

$$\omega_n = \frac{\Delta\theta}{\Delta t} = \frac{(\theta_{n+1} - \theta_n)}{\Delta t}$$

where $\Delta\theta$ is the change in rotation angle and $\Delta t$ is the change in time. $\Delta t$ remains constant at $6.25 \bullet 10^{-5}s$ since the data has been resampled to 16,000Hz. From $\omega_n$ the angular acceleration of the knee ($\alpha_n$) was calculated. The angular acceleration is defined as the change of the angular velocity with respect to time. Therefore, the instantaneous angular acceleration is the change in the angular velocity divided by the change in time:

$$\alpha_n = \frac{\Delta\omega}{\Delta t} = \frac{(\omega_{n+1} - \omega_n)}{\Delta t}$$

Fig. 6 shows the calculated kinematic variables of the knee joint synchronised with the AE signal.

### 2.3. Data analysis

#### 2.3.1. Normalisation and cross-correlation

The synchronised AE signal with the kinematic variables (θ, $\omega_n$,

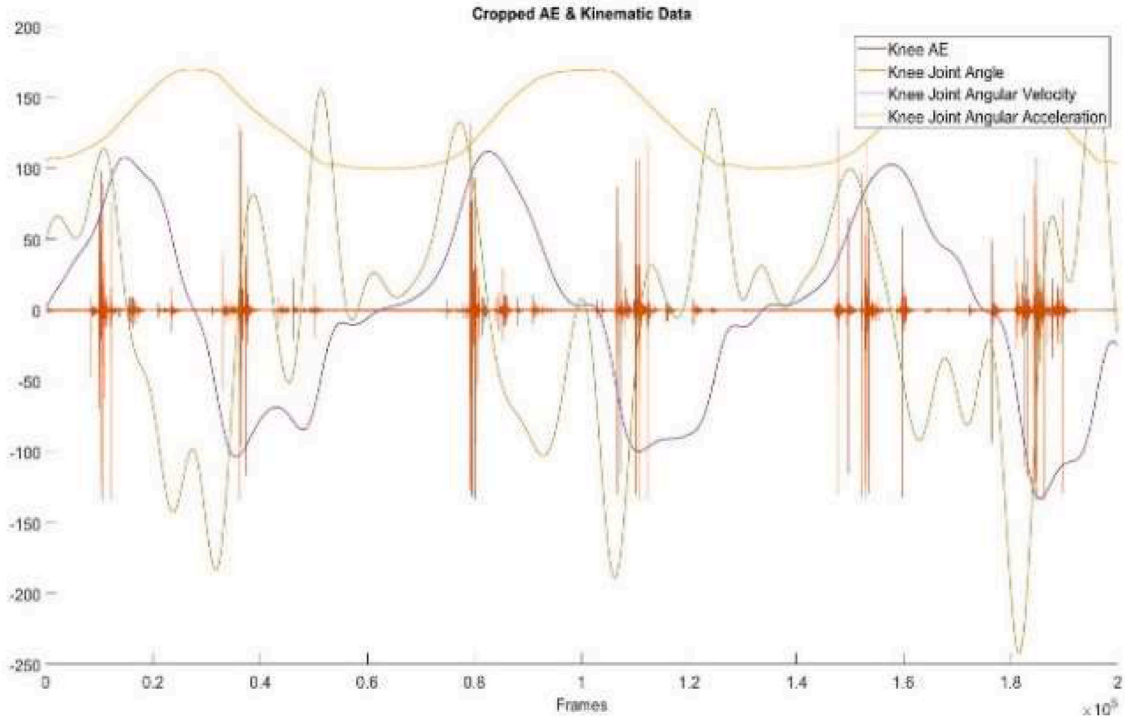


**Fig. 7.** The graph shows the cropped AE signal with the cropped kinematic variables.

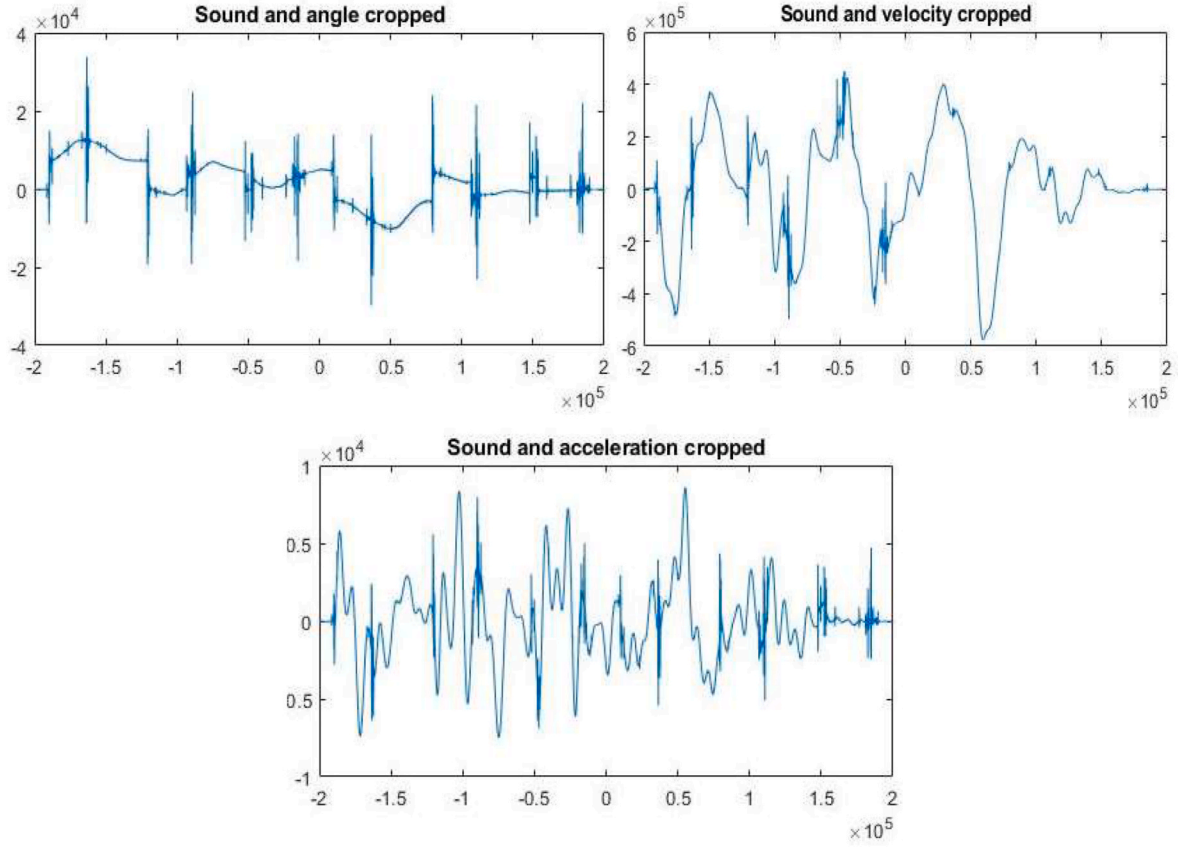


**Fig. 8.** The cross correlations between the AE signal and kinematic variables before applying the smoothing techniques. The cross-correlations show discontinuity (particularly in the cross-correlation with angle) due to fast oscillations between positive and negative values in the AE signal.

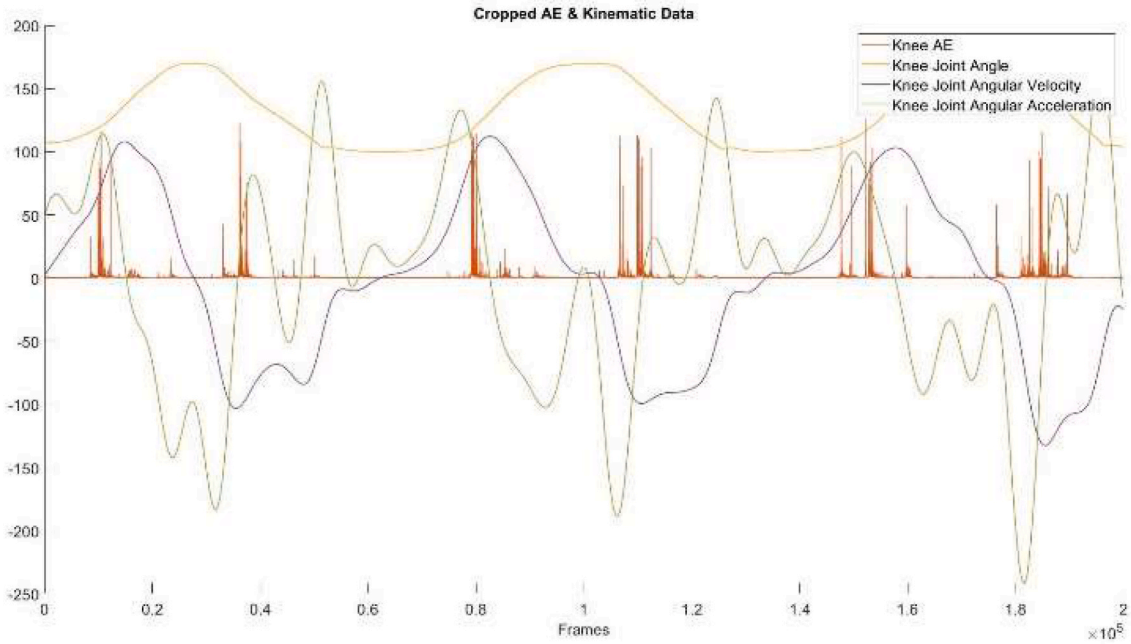


**Fig. 9.** Shows the AE signal after squaring, square rooting, and application of the moving average was carried out.

and$\alpha_n$) was cropped so only the relevant data (without the synchronizing taps) is used for further analysis. The cropped data were selected from the point where $\omega_n$ during the first S–S–S cycle was $> 0°s^{-1}$ and ended when the $\omega_n$after the last S–S–S was closest to $0\,°s^{-1}$(see Fig. 7). Since the Laryngograph had to be manually set up for every data collection, it was necessary to normalise the data to account for any measurement-to-measurement variations in channel sensitivity. More specifically, to normalise the AE data, the root-mean-square (RMS) level of the AE signal was calculated and then the AE signal was divided by this value to normalise the signal. This operation, as well as the remaining calculations, were carried out on the data sequences in Matlab™.

Cross correlation was carried out to measure the similarity between the AE signal and the dynamic signals. It was calculated as a function of the displacement in time (sliding product) of the AE signal relative to each of the dynamic signals. This was done to establish whether the acoustic signal is correlated with any of the kinematic variables (see Fig. 8). The three graphs show the cross-correlations carried out between the normalised AE data with the knee joint angle, angular

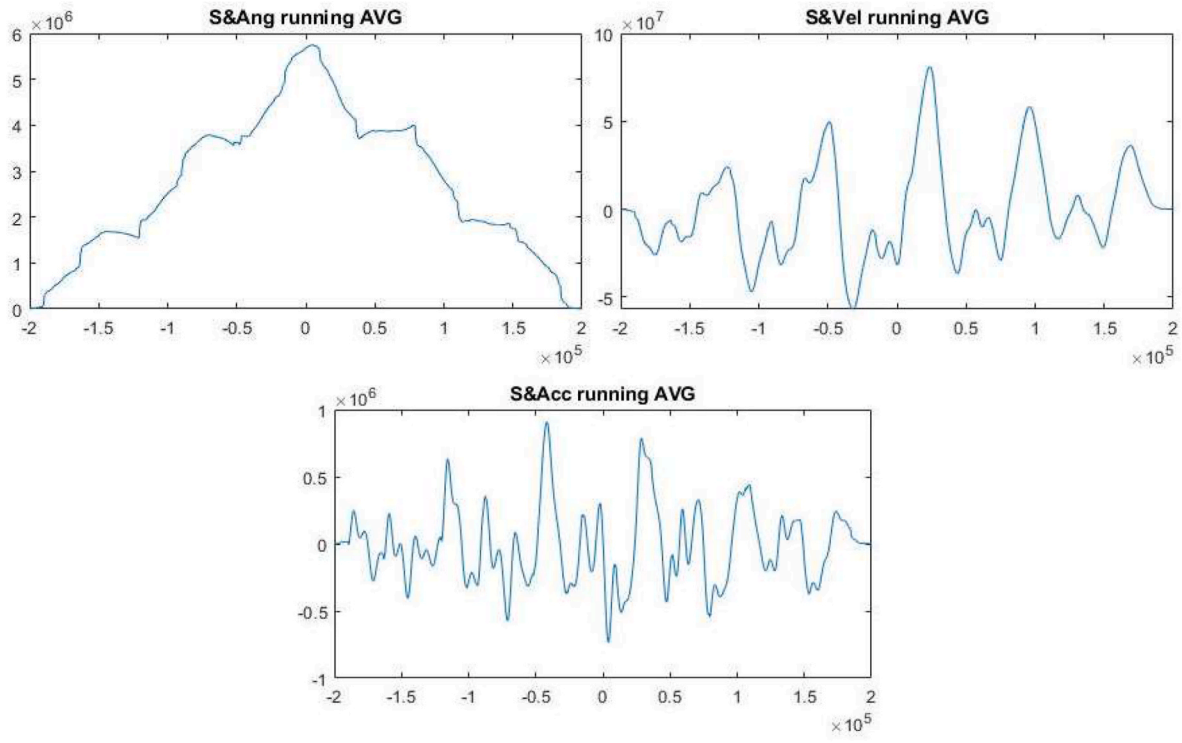


**Fig. 10.** Shows cross-correlation signals after 'smoothing' techniques were carried out.

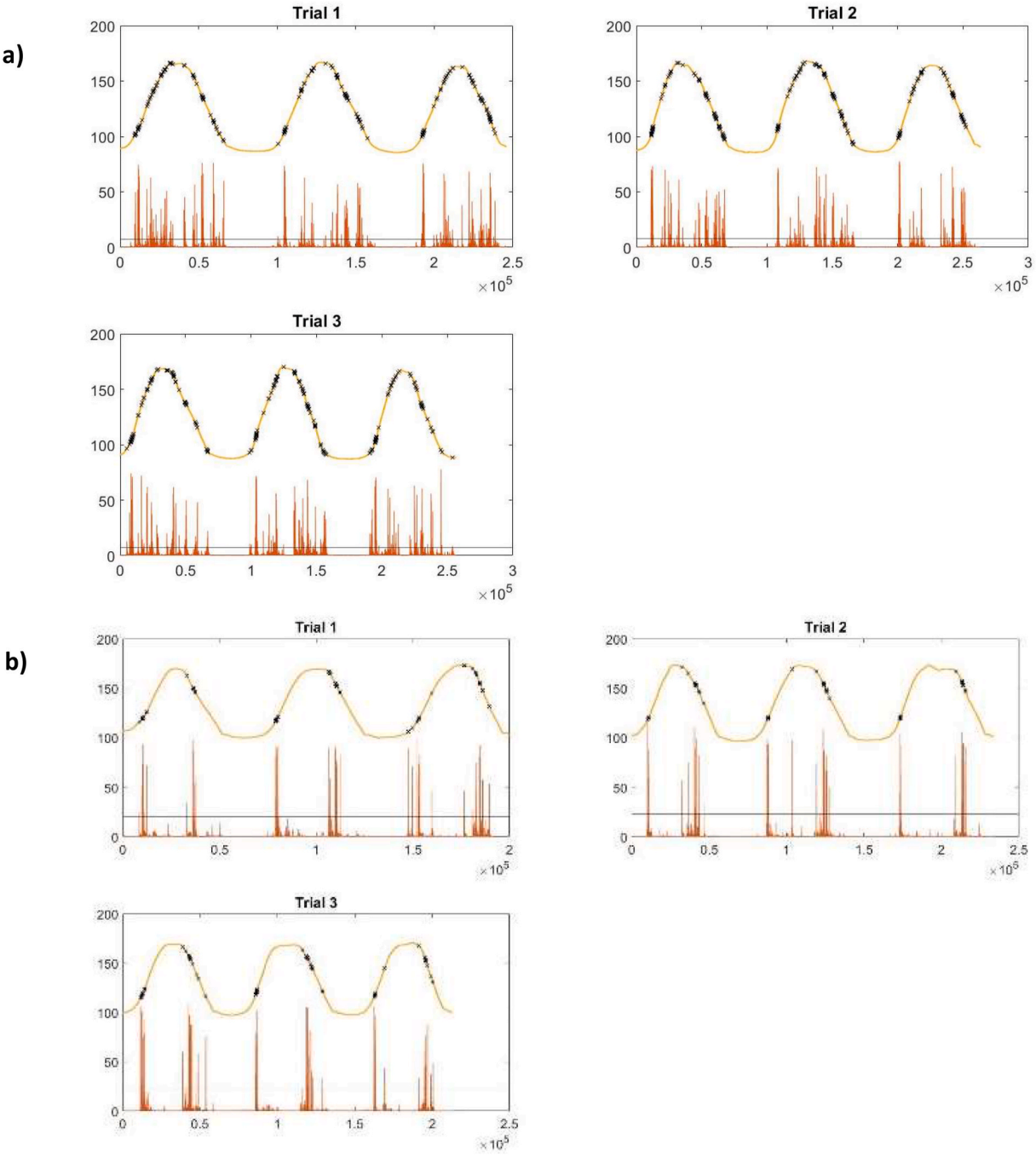


**Fig. 11.** The plots show the AE hits (AE values exceeding the threshold) with the locations of occurrence marked on the knee angle; a) a 'louder' knee b) a 'quieter' knee.

velocity, and the angular acceleration, respectively. A discontinuity in the cross-correlations was discovered; mostly noticeable in the AE and $\theta$ cross-correlations. Upon closer inspection of the signal, it was discovered that the apparent discontinuity is cause by fast oscillations between large positive and negative values of the AE signal whilst the knee angle signal was increasing and decreasing very gradually as can be seen in Fig. 7 (the orange line).

### 2.3.2. *Smoothing*

To eliminate the apparent discontinuity in the cross-correlations it was necessary to remove the sudden large changes in the sign of the AE signal. Therefore, the AE data was squared and the positive square root taken. This converted the negative parts of the signal to positive values as can be seen in Fig. 9. Subsequently a moving average of the processed AE signal was calculated. Each mean was calculated over a sliding window of 5 points across adjacent values of the AE data. This boxcar technique was employed to smooth discontinuities in the cross correlations between the AE signal and the kinematic variables.

Once smoothing was carried out, the AE signal and dynamic variables were cross-correlated once more. Discontinuities were eliminated from the cross-correlation signals and revealed strong correlations especially between the AE signal and angular velocity of the knee joint (see Fig. 10.)

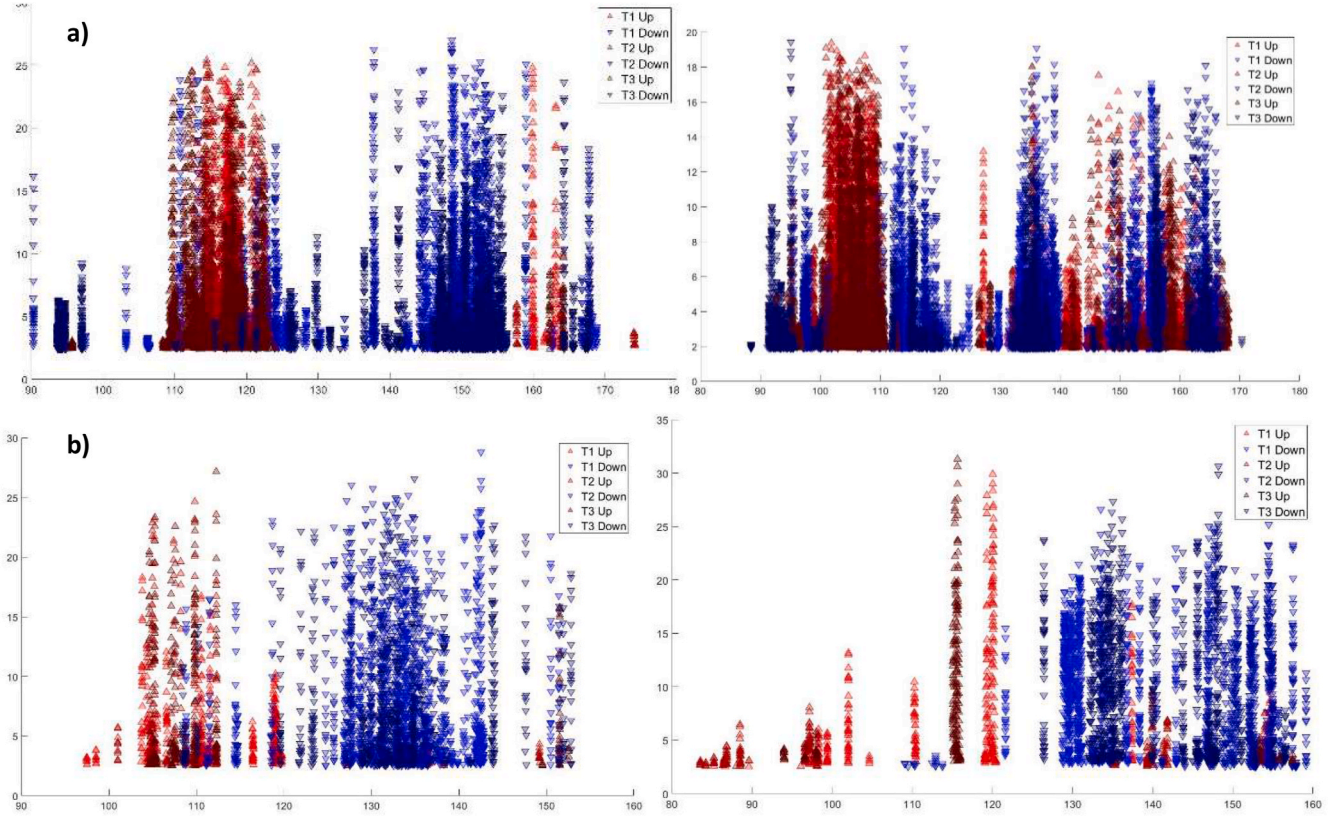


**Fig. 12.** The figure shows examples of scatter plots of a) 'louder' knees and b) 'quieter' knees. The clusters of the AE hits are grouped together based on the angle location of occurrence; the red arrows indicate the upward movement (knee extension) and the blue arrows indicate the downward motion (knee flexion). (For interpretation of the references to colour in this figure legend, the reader is referred to the Web version of this article.)

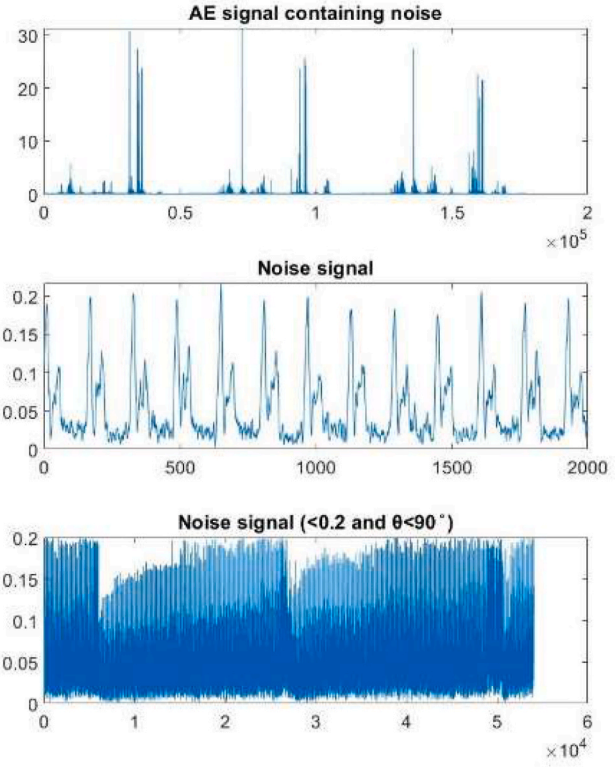


**Fig. 13.** The figure shows the signal noise components a) full AE signal containing noise b) noise (first 2000 frames) c) noise ($\theta < 90^{\circ}$ and signal strength <0.15).

## 3. Results

### 3.1. Identification of acoustic events and correlation with angle

Following the processing and cropping of the signals, the next stage was to identify the threshold for AE events (hits). For this another MATLAB™ code was developed. This procedure was carried out to isolate real signals from the noise or spurious values. The reason for doing this is so that this then permits the production of a scatter graph between the AE events and corresponding angles, angular speeds or angular accelerations. This procedure eliminated the time-dependence of the motion and established whether the AE was primarily produced at particular angles, angular velocities and accelerations for any specific subject under test. A threshold value of 10% of the five maximum values in the AE signal for each individual measurement was determined, and any AE value exceeding this was identified as a hit. This was then highlighted on the $\theta$ curve to identify the specific locations of the AE hits (see Fig. 11).

This preliminary analysis pipeline is already beginning to present a potential 'signature' signal for each participant. This is indicated in the representative scatter plot of the three trials for one of the participants (see Fig. 12).

It is apparent that the AE seems to be produced primarily at specific angles.

To illustrate the distinction between the noise and the acoustic signal, as well as the difference between different subjects a discrete data distribution method was adopted, in which the signals are presented in the form of a histogram of frequency (counts) versus signal strength. Due to noise, most likely of an electrical origin, the total counts in the first 2–3 bins (corresponding to low signal values) were considerably higher than the counts in the bins for the rest of the signal (see Fig. 13).

Therefore, for ease of comparison and to enable a more illustrative

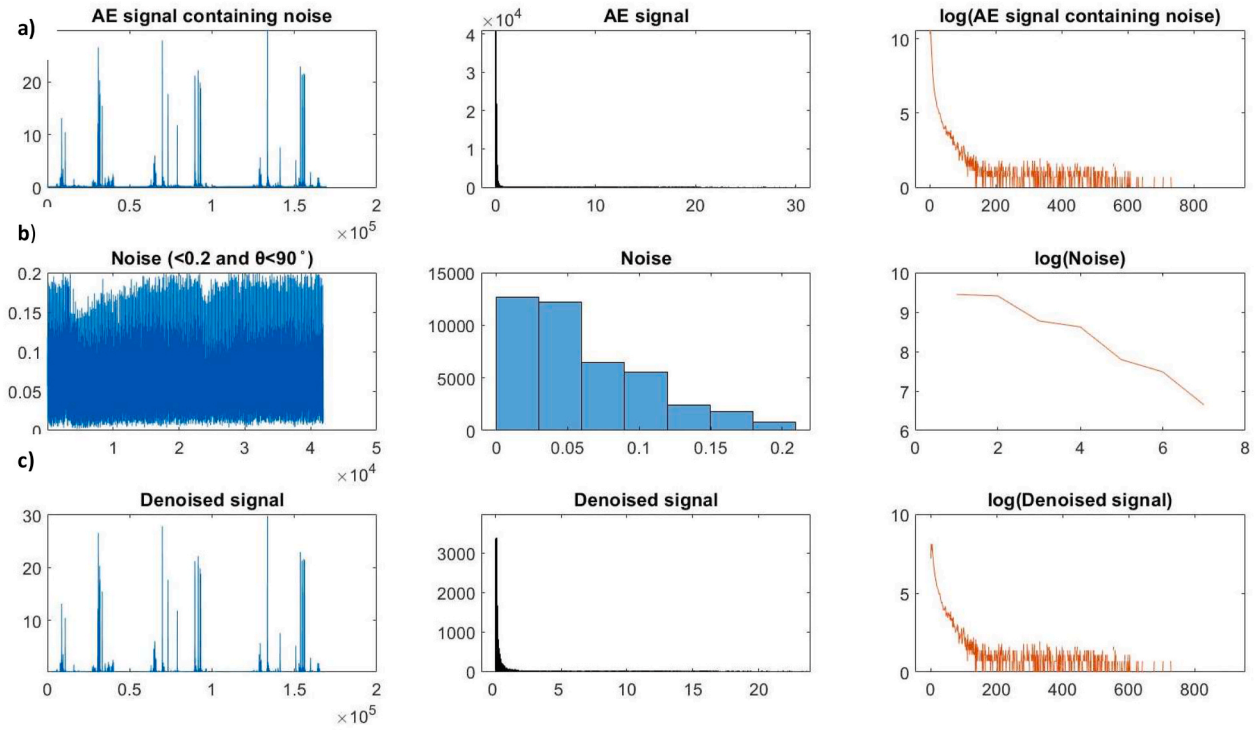


**Fig. 14.** The figure shows data distributions of a) full AE signal b) no movement AE signal c) adjusted bin counts AE signal.

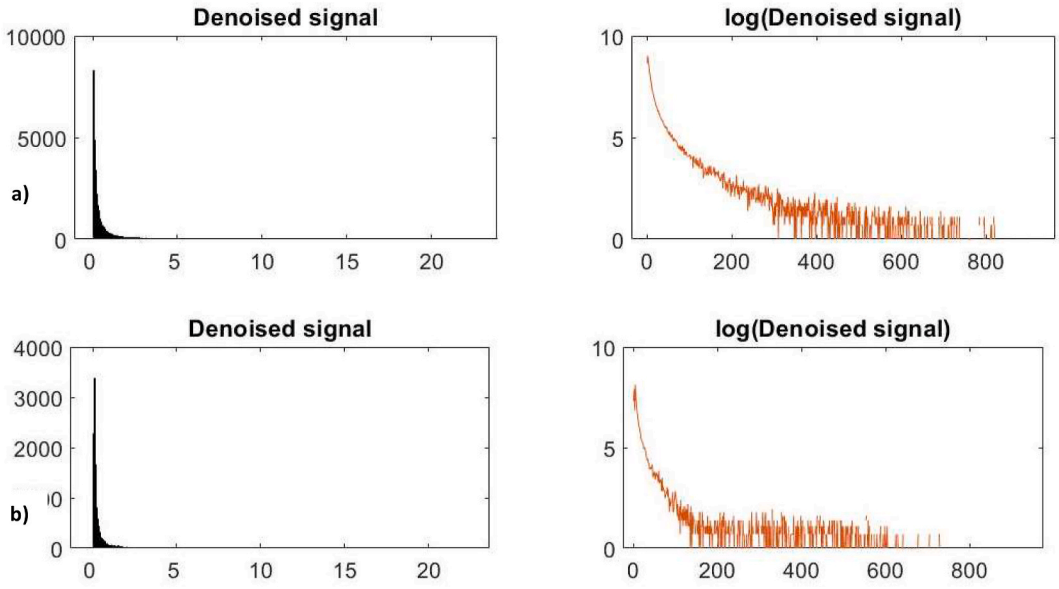


**Fig. 15.** The figure shows denoised data distributions of a) a 'loud' knee b) a 'quieter' knee.

display of counts across the full signal range the logarithm of the frequency was used to highlight the data distribution (see Fig. 14). Furthermore, in order to gain a more accurate representation of the noise contribution to the signal a sample of the signal was used where no movement occurred (defined as when the signal fulfilled both conditions $\theta < 90°$and signal strength $< 0.15$ dB) was selected. The bin counts were calculated and then scaled to match the full signal, which takes into account the fact that the bin counts are taken over a limited length of sample. This was done by calculating the ratio of the number of frames of the full AE signal to the number of frames of the 'no movement' (i.e. noise) AE signal. The bin counts evaluated for the noise signal were then multiplied by the ratio and subsequently subtracted from the full AE signal. This is then represented as the 'denoised signal'.

Fig. 15 shows the difference between the denoised data distributions for louder and quieter knees. As expected, the steepness of the slope in the 'loud' knees is visibly smaller than that of the knees with fewer AE hits.

## 4. Summary and conclusion

We have developed an operational multi-modal system that records simultaneously acoustic, kinematic, and dynamic data during a repeated Sit-Stand-Sit protocol by subjects and have recorded data for 15 consenting test subjects. A data analysis pipeline has been developed that

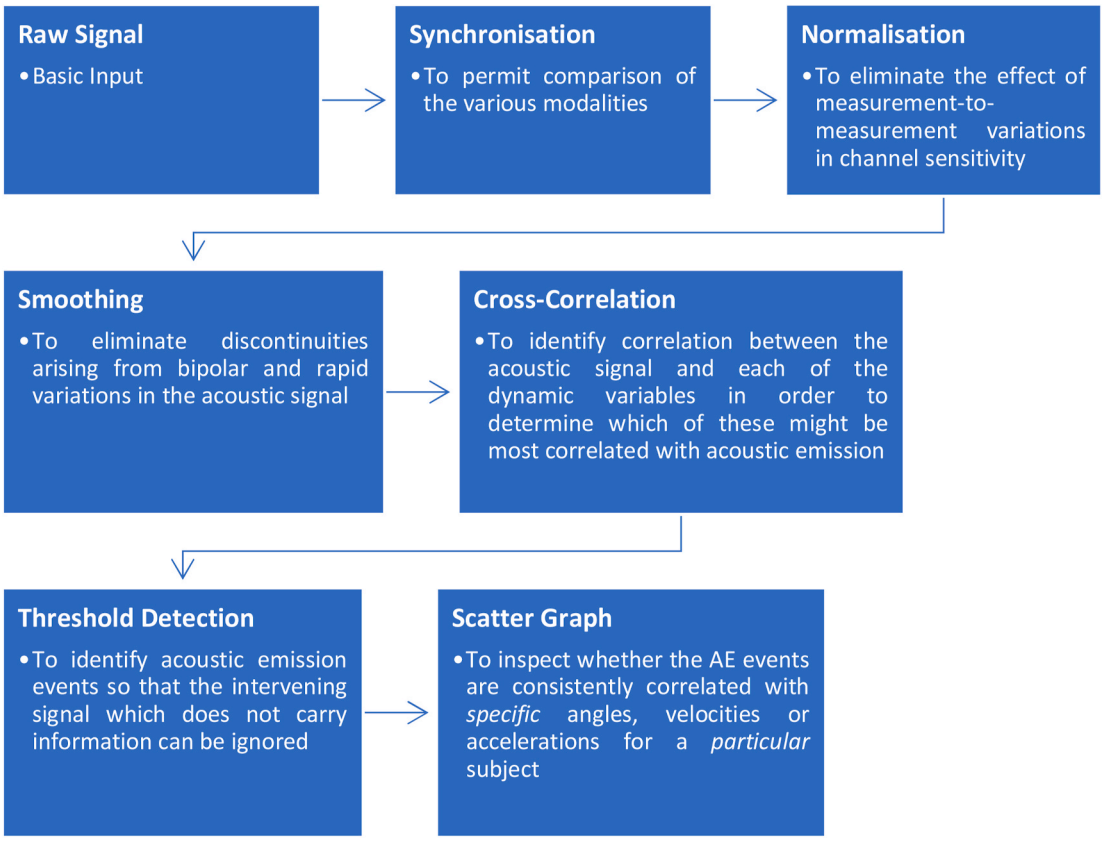


**Fig. 16.** A flow chart showing the steps in data processing.

displays the correlation between the production of acoustic events and, in this case, specific knee joint angles (see Fig. 16).

The development of such a protocol is considered to be a useful contribution as it is widely recognized that the recording of AE signals from knee joints is both difficult and inconsistent [22]; and see for example [23], and it is to be hoped that this procedure is a step towards the eventual standardisation of these measurement protocols.

Future work will include further processing of the data recorded, as well as the investigation of markers within these processed signals to distinguish between healthy and damaged knees and their dependence on the primary variables of age, gender, BMI, prior knee trauma, disease, and recent activity.

## CRediT authorship contribution statement

**I. Vatolik:** Conceptualization, Methodology, Investigation, Writing – review & editing, Software, Resources, Data curation, Formal analysis, Visualization, Writing – original draft. **M. Everington:** Conceptualization, Methodology, Investigation, Writing – review & editing, Software, Resources, Data curation. **G. Hunter:** Conceptualization, Methodology, Investigation, Writing – review & editing, Formal analysis, Project administration, Supervision. **N. Swann:** Conceptualization, Methodology, Investigation, Writing – review & editing, Formal analysis, Project administration, Supervision. **A.T. Augousti:** Conceptualization, Methodology, Investigation, Writing – review & editing, Software, Formal analysis, Visualization, Writing – original draft, Project administration, Supervision.

## Declaration of competing interest

The authors declare that they have no known competing financial interests or personal relationships that could have appeared to influence the work reported in this paper.

## References

[1] F. Eckstein, M. Tieschky, S. Faber, Functional analysis of articular cartilage deformation, recovery and fluid flow followig dynamic exercise in vivo, J. Anatomy Embryol. 200 (1999) 419–424.
[2] E. Hohmann, K. Wortler, A. Imhoff, MR imaging of the hip and knee before and after marathon running, Am. J. Sports Med. 32 (1) (2004) 55–59.
[3] M. Kessler, C. Glaser, S. Tittel, M. Reiser, A. Imhoff, Recovery of the menisci and articular cartilage of runners after cessation of exercise: additional aspects of in vivo investigation based on 3-dimensional magnetic resonance imaging, Am. J. Sports Med. 36 (5) (2008) 966–970.
[4] V. Mow, W. Hayes, Basic Orthopaedic Biomechanics, Lippincott-Raven, New York, 1997.
[5] F. Eckstein, B. Lemberger, C. Gratzke, M. Hudelmaier, C. Glaser, K. Englmeier, M. Reiser, In vivo cartilage deformation after different types of activity and its dependence on physical training status, Ann. Rheum. Dis. 64 (2005) 291–295.
[6] V. Silverwood, M. Blagojevic-Bucknall, C. Jinks, J.L. Jordan, J. Protheroe, K. P. Jordan, Current evidence on risk factors for knee osteoarthritis in older adults: a systematic review and meta-analysis, Osteoarthritis Cartilage 23 (4) (2015) 507–515.
[7] M. Blagojevic, C. Jinks, A. Jeffrey, K.P. Jordan, Risk factors for onset of osteoarthritis of the knee in older adults: a systematic review and meta-analysis, Osteoarthritis Cartilage 18 (1) (2010) 24–33.
[8] J. Showery, N. Kusnezov, J. Dunn, J. Bader, J. Belmont, B. Waterman, The rising incidence of degenerative and posttraumatic osteoarthritis of the knee in the United States military, J. Arthroplasty 31 (10) (2016) 2108–2114.
[9] A. Krampikowska, R. Pala, I. Dzioba, G. Swit, The use of the acoustic emission to identify crack growth in 40CrMo steel, Materials 12 (13) (2019) 2140.
[10] B. Mascaro, J. Prior, L. Shark, J. Selfe, P. Cole, J. Goodacre, Exploratory study of a non-invasive method based on acoustic emission for assessing the dynamic integrity of knee joints, Med. Eng. Phys. 31 (2009) 1013–1022.
[11] L. Shark, H. Chen, J. Goodacre, Discovering differences in acoustic emission between healthy and osteoarthritic knees using a four-phase model of sit-stand-sit movements, Open Med. Inf. J. 4 (2010) 116–125.
[12] D. Choi, S. Ahn, J. Ryu, M. Nagao, Y. Kim, Knee acoustic emission characteristics of the healthy and the patients with osteoarthritis using piezoelectric sensor, Sensor. Mater. 30 (8) (2018) 1629–1641.
[13] C. Teague, S. Hersek, H. Toreyin, M. Millard-Stafford, M. Jones, G. Kogler, M. Sawka, O. Inan, Novel methods for sensing acoustical emissions from the knee for wearable joint health assessment, IEEE (Inst. Electr. Electron. Eng.) Trans. Biomed. Eng. 63 (8) (2016) 1581–1590.

[14] F. Charkravarty, H. Hubert, V. Lingala, E. Zatarian, J. Fries, Long distance running and knee osteoarthritis. A prospective study, Am. J. Prev. Med. 35 (2) (2008) 133–138.
[15] J. Bijlsma, K. Knahr, Stretegies for the prevention and management of osteoarthritis of the hip and knee, Best Pract. Res. Clin. Rheumatol. 21 (2007) 59–76.
[16] D. Felson, An Update on the Pathogenesis and Epidemiology of Osteoarthritis, vol. 42, Radiologic Clinics of North America, 2004, pp. 1–9.
[17] D. Felson, Osteoarthritis: new insights. Part 1: disease and its risk factors, Ann. Intern. Med. 133 (2000) 635–646.
[18] G. Ateshian, W. Lai, W. Zhu, V. Mow, An asymptotic solution for the contact of two biphasic cartilage layers, J. Biomech. 27 (1994) 1347–1360.
[19] D. Moschella, A. Blasi, A. Leardini, A. Ensini, F. Catani, Wear patterns on tibial plateau from varus osteoarthritis knees, Clin. BioMech. 21 (2006) 152–158.
[20] K. Kręcisz, D. Bączkowicz, Analysis and multiclass classification of pathological knee joints using vibroarthrographic signals, Comput. Methods Progr. Biomed. 154 (2018) 37–44.
[21] C. Frank, R. Rangayyan, G. Bell, Analysis of knee joint sound signals for non-invasive diagnosis of cartilage pathology, IEEE Eng. Med. Biol. Mag. 9 (1) (1990) 65–68.
[22] K.L. Richardson, S. Gharehbaghi, G.C. Ozmen, M.M. Safaei, O.T. Inan, Quantifying signal quality for joint acoustic emissions using graph based spectral embedding, IEEE Sensor. J. (2021) 99, 1-1.
[23] D. Cheneler, Diagnosing arthritic knees using vibration UK biomedical acoustics SIG seminar 26th June 2020. https://www.ioa.org.uk/uk-biomedical-acoustics-sig-webinar-26th-june-2020, 2020.
[32] G. McCoy, J. McCrea, D. Beverland, W. Kernohan, R. Mollan, Vibration arthrography as a diagnostic aid in diseases of the knee. A preliminary report, J. BonenJoint Surgery-British 69 (1987) 288.
[37] L. Shark, H. Chen, J. Goodacre, Knee acoustic emission: a potential biomarker for quantitative assessment of joint ageing and degeneration, Med. Eng. Phys. 33 (2010) 534–545.